Asian Journal of Chemistry; Vol. 34, No. 9 (2022), 2331-2336

ASIAN JOURNAL OF CHEMISTRY

https://doi.org/10.14233/ajchem.2022.23872

Supramolecular Gels with Mouldable Properties from Fatty Acid to make Graphene-Based Nanohybrid Paper

Abhijit Biswas

Department of Chemistry, Krishnagar Government College, Krishnagar, Nadia-741101, India

Corresponding author: E-mail : biswas.abhijit5@gmail.com

Received: 20 April 2022; *Accepted*: 23 June 2022; *Published online*: 19 August 2022; AJC-20930

"Paper-like" materials composed of graphene exhibit good mechanical, thermal and electronic properties and are expected to find a variety of applications. Herein, a simple and elegant strategy has been reported to obtain a graphene-based nanohybrid paper. Mysristic acid in sodium salt-containing aqueous solution forms a stable hydrogel. When myristic acid was mixed with glucose and graphene oxide produces graphene-based gel under the treatment of heating and subsequent cooling through electrostatic stabilization. By applying proper mechanical compression on gel a stable and flexible nanofibrillar graphene-based paper has been obtained without destroying the network structure. This study has enabled to develop of a facile approach to large-scale production of graphene-based paper. The properties of this graphene-based paper have been investigated using electron microscopy, FT-IR spectroscopy, X-ray diffraction and Raman spectroscopy. The obtained paper is thermally stable and resistant to a wide range of organic solvents and therefore interesting in making various advanced electronics.

Keywords: Hydrogel, Self-assembly, Graphene, Nanohybrid paper.

INTRODUCTION

Two-dimensional honeycomb nanostructure based graphene has an intrinsic electronic conductivity, high strength and stability, low cost and a large surface area [1-4]. This unique nanostructure holds great promise for potential applications in many technological fields such as nanoelectronics, nanocomposites, sensors, batteries, supercapacitors and hydrogen storage [5]. However, stabilizing graphene in aqueous media has been a major obstacle to exploit the most proposed applications. The high specific surface area and lack of presence of sufficient hydrophilic groups of graphene tend to form agglomerates or precipitates in an aqueous medium.

Graphene oxide (GO) obtained from graphite and contains a range of functional groups, such as hydroxyl and carboxylic acid groups at the edges, which make the GO hydrophilic [6,7]. Therefore, GO can be easily dispersed in the aqueous solution. But, GO is electrically insulating and thermally or mechanically less stable compared to graphene and can be converted to graphene by chemical reduction, for example, using ascorbic acid, hydrazine and glucose in the aqueous medium. But in such a procedure graphene starts to agglomerate and appears to be insoluble in an aqueous solution. The prevention of aggregation is of particular importance for graphene sheets because most of their unique properties are only associated with individual sheets. Stabilization of graphene can be obtained by the attachment of other molecules or polymers onto the sheets [8,9]. On the other hand, hydrogel comprised of gelator molecules and solvent holds great promise for the potential stabilization of carbon based nanomaterials nanomaterials [10,11]. For example, Banerjee *et al*. [12] reported an amino acid based hydrogel that can stabilize a variety of carbon based nanomaterials, including graphene oxide, graphene, and pristine single-walled carbon nanotubes. Sui *et al*. [13,14] made a significant contribution to graphene-based gels. There have been several other reports on GO and graphene based gel [15-19]. Recently, Shi *et al*. [20] described a highly conductive, thermally stable self-assembled graphene hydrogel and used it as an electrode for supercapacitors. However, for potential applications in technological fields such as nanoelectronics, sensors, nanocomposites, batteries, supercapacitors and hydrogen storage, paper or film like material is more advantageous over gel due to the thin dimension and flexibility of paper or film [21]. Such properties of film or paper lead to many synthesis techniques for graphene-based film/paper [2-4]. Cheng *et al*. [22] developed flexible graphene/polyaniline composite paper by *in situ* anodic electropolymerizations and used it as self-standing flexible electrodes for supercapacitors [22]. Seppälä *et al*. [23] successfully prepared graphene/cellulose nanocomposite paper that shows an excellent electrical property with high mechanical strength. Xia *et al*. [24] have reported a graphene sheet/porous NiO hybrid film to improve pseudocapacitive behavior of the sample. Subsequently, several graphene-based papers or films have been found in the literature [25-28].

In this report, a simple strategy has been developed to obtain graphene based paper. Myristic acid produces a stable hydrogel in a 1 M $NaHCO_3$ solution. It has been found in the literature that glucose can reduce GO to graphene [29]. The hydrogel comprised of myristic acid, glucose and aqueous GO leads to the formation of graphene based nanohybrid hydrogel. The graphene is well stabilized into the gel matrix. By applying the mechanical pressure, gel forms a stable nanohybrid paper without destroying the network structure. Such an environment friendly strategy enables the simple and most convenient method of making graphene based nanohybrid paper. The nanohybrid paper is highly flexible and exhibits good stability in a range of common organic solvents for a long time.

EXPERIMENTAL

The chemicals *viz*. H_2SO_4, $KMnO_4$, sodium nitrate, H_2O_2, all fatty acids, ammonia and solvents were purchased from SRL, India. Graphite powder was purchased from Sigma-Aldrich, India. Ultra pure Milli-Q grade water was used in all experiments.

Preparation of graphene oxide (GO): Graphene oxide (GO) was synthesized from natural graphite powder (< 30 µm) according to modified Hummers & Offeman's method [30].

Hydrogel preparation: A self-supporting translucent hydrogel was obtained in 1 M $NaHCO_3$ solution. In a typical experiment, a definite amount of gelator, myristic acid (0.56 mg) was taken in a glass vial along with 1 M $NaHCO_3$ solution (1.5 mL). The mixture was heated at 65 ºC to form a clear solution. Then, this solution was settled down at room temperature for few minutes to obtain a self-supported translucent hydrogel (Fig. 1). The gel formation was confirmed by vial-inversion method. The minimum gelation concentration (MGC) of the gelator has been found to be 0.035 % (w/v).

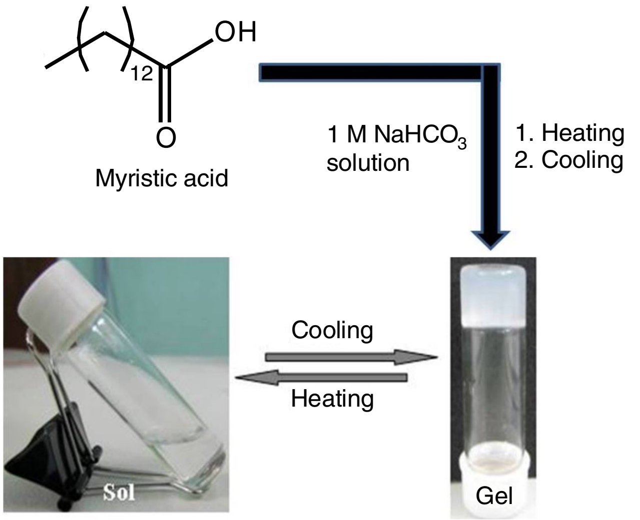

Fig. 1. Optical image of hydrogel obtained from myristic acid in 1 M $NaHCO_3$ solution and switching of gel to sol state. The concentration of the gelator in the hydrogel is 0.05% (w/v)

Characterization: X-ray diffraction of dried paper was carried out in X-ray diffractometer (Bruker D8 Advance) equipped with a conventional Cu$K\alpha$ X-ray radiation (λ = 1.54 Å) source and Bragg diffraction setup (Seifert 3000P). TGA measurement was performed using a TA SDT Q600 instrument at a heating rate of 10 ºC min^{-1} under a nitrogen atmosphere. For Raman spectra, the graphene-based nanohybrid paper (powder condition) was placed on the surface of a glass slide. The sample was dried at room temperature prior to the measurement. Raman spectra were recorded by irradiating with laser light at 632.81 nm in a Horiba Jobin Yvon instrument (LABRAM HR 800). For FE-SEM studies, the powdered paper was dispersed in water by sonication. The small portion of dispersed solution was placed on a microscope cover glass. Then, these sample was dried first in air and then in vacuum and coated with platinum for 90 s at 10 kV voltages and 10 mA current. Micro-graphs were recorded using a FE-SEM apparatus (Jeol Scanning Microscope-JSM-6700F). Transmission electron microscopic (TEM) experiments were carried out to investigate the morphology of nanohybrid paper. The powdered paper was dispersed in water by sonication. A drop of the dispersed solution was placed on carbon coated copper grids (300 mesh) and dried by slow evaporation. Each grid was then allowed to dry under vacuum at 30 ºC for two days. TEM images were recorded on a JEM 2010F electron microscope at an accelerating voltage of 200 kV.

RESULTS AND DISCUSSION

Gelation studies: Five types of fatty acids viz. capric acid, lauric acid, myristic acid, palmitic acid and stearic acid with linear alkyl chains 10, 12, 14, 16, and 18 methylene units have been used for their gelation behavior in aqueous (basic) media (Table-1). Out of these fatty acids, only myristic acid (carbon chain length 14) has shown stable hydrogel formation in an alkaline solution of sodium salts such as NaOH, $NaHCO_3$ and Na_2CO_3. Capric acid (carbon chain length 10) and lauric acid (carbon chain length 12) give a transparent solution and never formed gel even upon standing for long days under similar conditions. The fatty acid of carbon chain lengths 16 (palmitic acid) and 18 (stearic acid) has also been unable to form gel instead of the precipitate formation.

TABLE-1
GELATION STUDIES OF DIFFERENT
FATTY ACIDS IN 1 M $NaHCO_3$ SOLUTION

Fatty acids	Observation
Capric acid	Solution
Lauric acid	Solution
Myristic acid	Gel
Palmitic acid	Precipitation
Stearic acid	Precipitation

These observations suggested that the hydrogel formation depends on the carbon chain length of the fatty acid. The hydrogel is thermoreversible in nature *i.e*. the gel has been converted to the solution (sol) upon heating and again it gets back to the gel upon cooling at room temperature within a few minutes.

Salt effect on hydrogel formation: The thermal stability of hydrogel has been measured by determining the gel melting temperature (T_m), *i.e*. the temperature at which the gel is transformed into the solution (sol). The T_m values have been checked according to the test-tube inversion method. Fig. 2 represents the T_m *versus* gelator concentration plot. Hydrogel formation is also influenced by the concentration of salt present in the solution. In order to obtain more clear result, a stable hydrogel has been prepared in 1M $NaHCO_3$ solution [gelator concentration 0.037% (w/v)]. With the dilution of gel with water, it transformed into a viscous fluid and never formed gel under similar heating-cooling procedure. If now increase the sodium salt content of same fluid, *i.e*. by the addition of saturated $NaHCO_3$ solution, the viscous fluid form an opaque hydrogel (Fig. 3). It indicates a marked 'salt effect' during the gel formation and can be utilized to perform salt-induced supramolecular hydrogel formation. Contrary to sodium salt, it has been found that no gelation occurred in the corresponding lithium or potassium salts. This observation indicates that not only the content of salt but also the type of salt has a significant influence on gel formation. This sodium salt effect on the gel formation may be due to the stable bridging of sodium ions between carb-oxylate amphiphiles over lithium or potassium. Thus, sodium ion has assisted crosslinking of micellar assemblies of the sodium carboxylate amphiphiles and lead to hierarchical aggregation. Additionally, increasing sodium salt content means strengthening the hydrophobicity according to the Hofmeister series [31]. This also leads to enforced self-aggregation of the molecules.

Mouldability and load-bearing ability of hydrogel: The hydrogel has been prepared through non-covalent interactions and exhibits high mechanical strength with stability for a couple of months without losing any physical properties. The self-standing hydrogel can bear an exceptionally high load without any deformation. Fig. 4a represents the load-bearing ability of the hydrogel. In this experiment, a mass with a weight of 100 g has placed on top of the self-standing cylindrical type gel with a length of 1.6 cm, a diameter of 1.2 cm and a weight of 0.5 g. It means that the gel can easily bear approximately 8.7 kPa pressure without deformation. Additionally, the hydrogel exhibits excellent mouldable properties. In this regard, a solution of myristic acid in 1M $NaHCO_3$ has been poured into a template of a doll sculpture. On standing for a few minutes, it enables a sculpture of a doll that is stable for a couple of months (Fig. 4b).

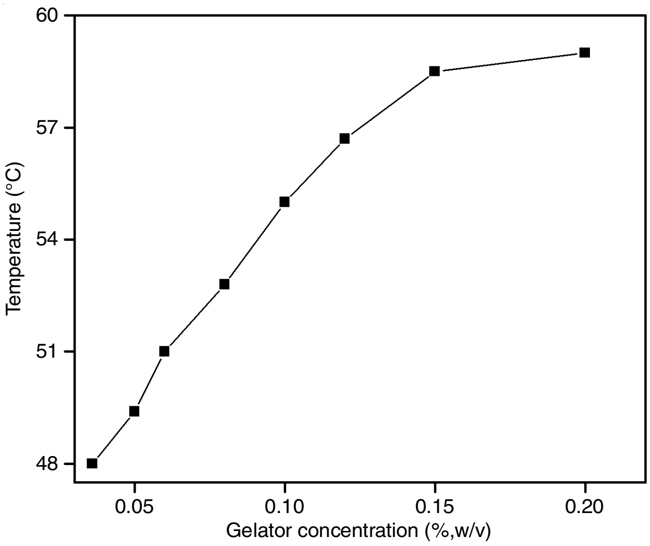

Fig. 2. Changing of gel melting temperatures (T_m) with respect to gelator's concentration in 1 M $NaHCO_3$ solution

Preparation of graphene-based nanohybrid hydrogel: Several water-soluble reducing reagents such as hydrazine, L-ascorbic acid and glucose for the reduction of GO has been reported. Among them, L-ascorbic acid and glucose offer an environmentally friendly approach for the large-scale production of water-soluble graphene. However, due to the lengthy experimental time required for L-ascorbic acid [32] here, the reduction procedure has been performed with glucose. In a typical experiment, at first, 1.5 mg of GO have dispersed in a 1 mL 1M $NaHCO_3$ solution. A mixture of myristic acid and glucose in 1M $NaHCO_3$ solution has been heated to melt into the solution state. Then, 0.2 mL of dispersed GO and a few drops of aqueous NH_3 solution has been added to the hydrogel solution in the glass vial and the resulting mixture has been

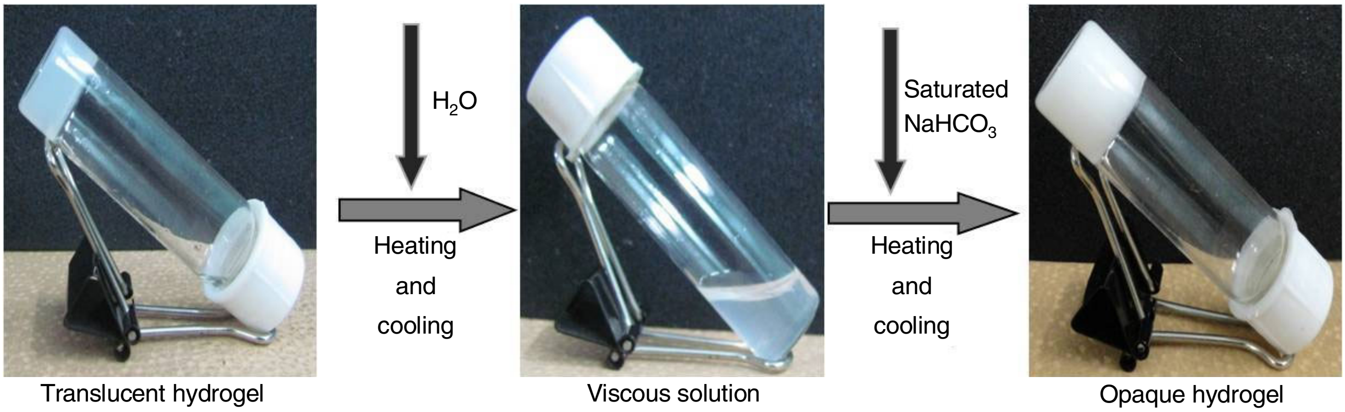

Fig. 3. Demonstration of salt-induced hydrogel formation

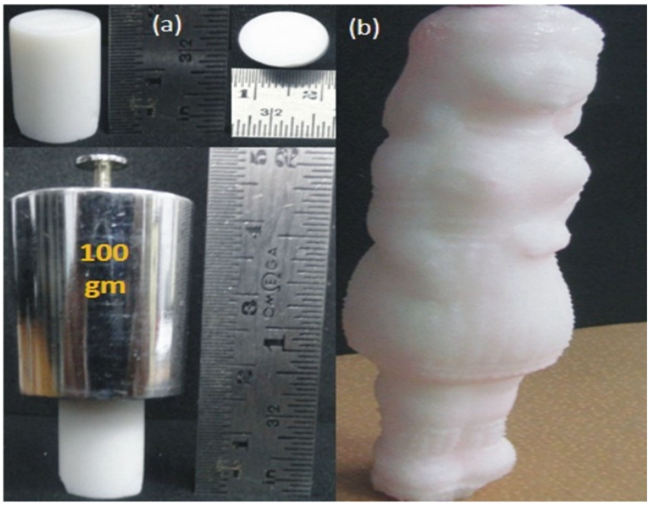

Fig. 4. (a) Load bearing ability of the hydrogel; (b) 'doll' sculpture formation of the hydrogel

heated to 95 ºC. The colour change of the solution (brownish yellow to black) indicates the reduction of GO to graphene. After cooling at room temperature it results in graphene containing hybrid hydrogel (Fig. 5). Thus, this approach (simultaneous reduction and stabilization of graphene into the gel matrix) provides an effective approach to making a graphene-based nanohybrid hydrogel.

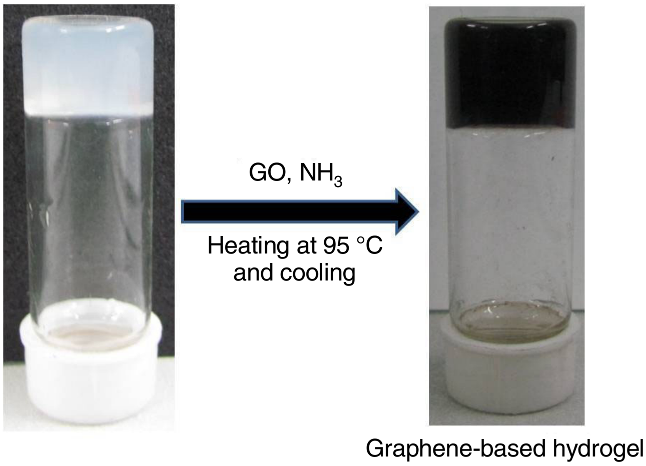

Fig. 5. Formation of graphene-based nanohybrid hydrogel

Preparation of graphene-based nanohybrid paper: It has been found that a stable nanofibrillar paper-like material can be obtained by applying proper mechanical compression on gel without destroying the network structure. At first, graphene containing hydrogel has been prepared in a glass Petri disk. The gel is sufficiently stable and has been placed completely on the top of a glass plate having a smooth surface area. Another glass Petri disc has been put on the gel. The whole setup is like a sandwich type. Gentle pressure has been applied to remove the solvent. Finally, it has been placed in a vacuum desiccator for about 2 h to remove traces amount of water. This procedure results in a self-supporting, free-standing, flexible graphene-based paper (Fig. 6). The dimension of nanohybrid paper has been measured. In gel condition, diameter and height were 4.5 cm and 1 cm, respectively which depends on the initial filling dimension of the Petri disc. After nanohybrid paper formation height reduces to 0.16 mm without alteration of diameter. The nanohybrid paper exhibits sufficient stability against a wide range of solvents. Stability has been tested by dipping it into the solvents at room temperature. It has been observed that nanohybrid paper possessed sufficient stability against various organic solvents, such as chloroform, THF, DCM, toluene, methanol, xylene, hexane, acetone and ethyl acetate. At a low pH, this nanohybrid paper material has also kept its integrity at room temperature. However, the paper is unstable in Na_2CO_3 or NaOH solution. The whole observations have been summarized in Table-2. Apart from the solvent stability, the nanohybrid paper has also remarkable thermal stability. The thermogram curve (Fig. 7a) shows the small weight loss (~3%) occurs at lower temperatures. This weight loss is due to the presence of a very little amount of water in the sample. Considerable a weight loss (70.1%) occurs only at higher temperatures (~ 380 °C) implying that the paper is stable up to 380 ºC. The higher thermostability of the nanohybrid paper is attributed to the combination of a shorter hydrophobic alkyl chain and strong intermolecular interactions.

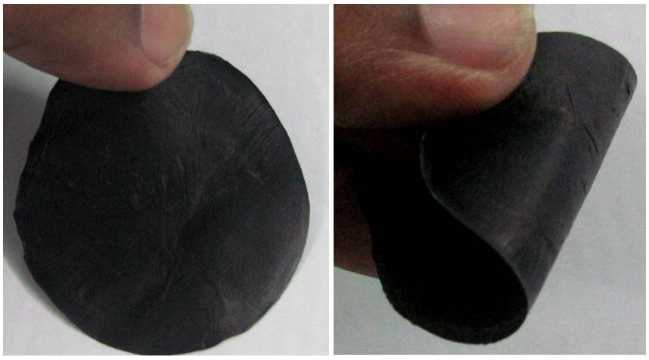

Fig. 6. Camera view of graphene-based nanohybrid paper

TABLE-2
CHECKING OF STABILITY OF GRAPHENE-BASED NANOHYBRID PAPER IN DIFFERENT SOLVENTS

Solvent	Observation
Organic solvents (THF, DCM, chloroform, toluene, methanol, xylene, hexane, acetone and ethyl acetate)	Stable
1 M HCl	Stable
Aqueous solution of pH 4, pH 5 and pH 5.5	Stable
Millipore water	Stable
1 M NaOH, 1 M $NaHCO_3$, 1 M Na_2CO_3	Unstable

FT-IR studies: In Fig, 7B, a peak at 1705 cm^{-1} is due to the symmetric stretching frequency of carboxyl carbon of myristic acid. The shift of frequency in the lower region (1559 cm^{-1} for graphene-based paper) indicates the good interaction of graphene with gelator molecules.

XRD studies: The XRD analysis of the dried paper shows a stronger diffraction pattern. The 2θ values of the sample appear at 4.90º, 7.40º, 9.79º, 12.30º and 22.81º (Fig. 8). The ratio of 2θ values (2:3:4:5:9) indicates the highly ordered multilayer structures of the paper. In the graphene based paper, an additional broad diffraction peak at approximately 2θ = 24.5°

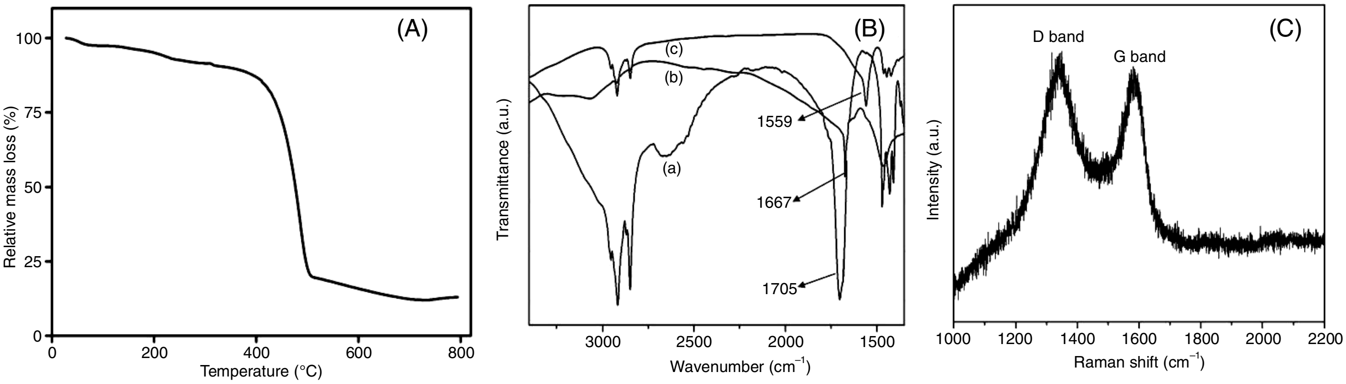

Fig. 7. (A) TGA curve of graphene-based nanohybrid paper; (B) FT-IR spectra of (a) myristic acid, (b) hydrogel (dried condition) and (c) graphene-based paper; (C) Raman spectrum of graphene-based sample

has been observed (Fig. 8). This corresponds to the typical 002 planes (*d*-spacing of around 0.36 nm) of the graphene [33]. This result implies the good stabilization of graphene in the graphene based paper.

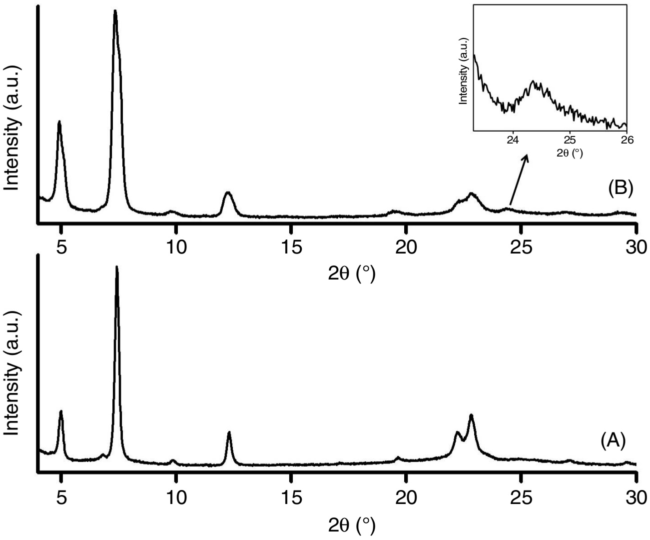

Fig. 8. XRD pattern of (A) hydrogel and (B) graphene-based paper

Raman studies: Raman spectroscopy is a tool to determine the microstructure of carbon-based materials. The G-band derives intensity from carbon-carbon double bond stretching vibrations and the D-band derives intensity from bending vibrational modes associated with C-O bending modes [32,34]. Raman spectrum analysis of dried graphene-based nanohybrid paper show two fundamental vibrations at 1343 and 1584 cm^{-1} correspond to the D band and G band, respectively (Fig. 7c). The higher intensity ratio of D/G bands (more *sp*^{2} domain) compared to that of pristine graphite or GO suggests the presence of graphene in graphene-based paper.

Morphological characterizations: Morphologies of the nanohybrid paper have been studied through field emission scanning electron microscopy (FE-SEM) and transmission electron microscopy (TEM). Figs. 9a and 9b represent the respective FE-SEM image and TEM image of graphene-based nanohybrid material. Both images show the presence of nanofibers. These fibrils are several micrometers in length and average width of 22 nm. In addition to nanofibrillar network structure nanosheets of graphene have also been obtained. Interestingly, it has been found that fibrils form a crosslinked network nature and it is mostly positioned on the graphene nanosheet surface suggesting the presence of a nanohybrid system comprised of

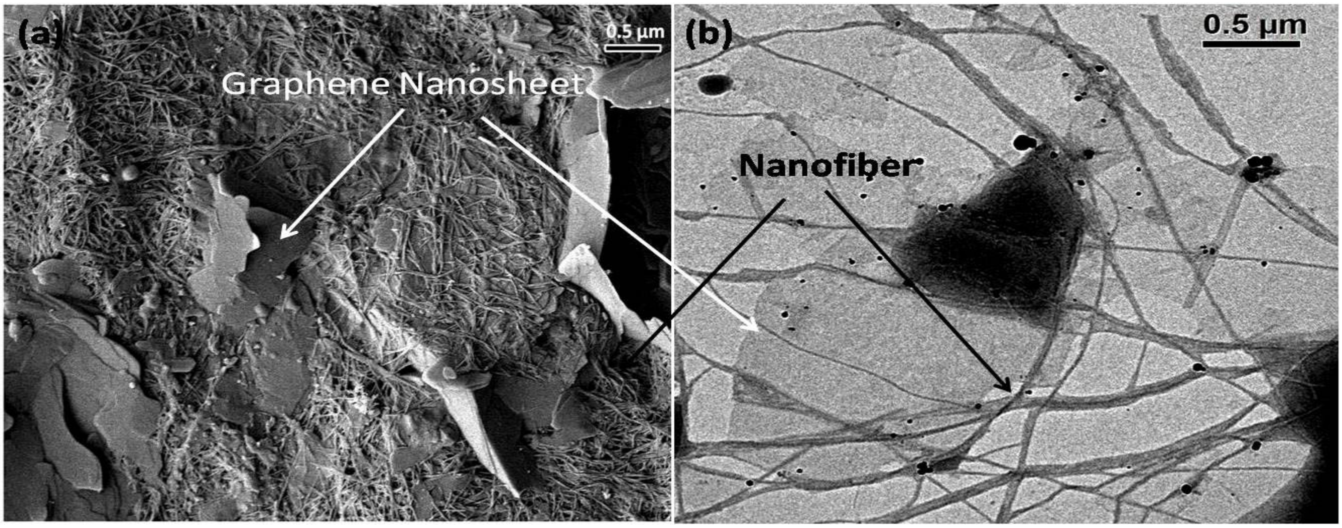

Fig. 9. (a) FE-SEM image and (b) TEM image of graphene-based nanohybrid paper

nanosheets and nanofibers. The uniformity of these supramolecular aggregates in these studies suggests that each of these molecules has self-assembled in a hierarchical fashion to provide a larger network of superstructures.

Conclusion

In conclusion, it can be said that a simple, procedure has been developed for the large-scale preparation of graphene-based nanohybrid paper, which is based on the self-assembly process of fatty acid in an alkaline solution. Myristic acid mixed with glucose and graphene oxide in sodium salt containing alkaline solution forms graphene oxide containing hydrogel that can be transformed to a graphene-based nanohybrid hydrogel by the treatment of simultaneous heating and cooling. Using appropriate mechanical pressure, the gel can form a stable, flexible and free-standing soft paper. The nanohybrid paper has the potential to resist a range of common organic solvents and also exhibits good thermal stability. The properties of this graphene based paper have been investigated using electron microscopy (FE-SEM and TEM) and spectroscopy (such as FT-IR, Raman spectroscopy and X-ray diffraction). All these experimental results imply the considerable stabilization and interactions of graphene in the graphene-based nanohybrid paper. This simple and most reliable method holds great promise for the creation of advanced graphene-based materials for high-tech electronic applications such as transplant devices, invasive instruments, portable and bendable electronics.

ACKNOWLEDGEMENTS

The author gratefully acknowledges Krishnagar Government College, Krishnagar, India for providing the research facilities. Thanks are also due to Indian Association for the Cultivation of Sciences (IACS), India for providing the instrumental facilities and library.

CONFLICT OF INTEREST

The authors declare that there is no conflict of interests regarding the publication of this article.

REFERENCES

1. D.H. Lee, J.E. Kim, T.H. Han, J.W. Hwang, S. Jeon, S.Y. Choi, S.H. Hong, W.J. Lee, R.S. Ruoff and S.O. Kim, *Adv. Mater.*, **22**, 1247 (2010); https://doi.org/10.1002/adma.200903063
2. K. Yu, P. Wang, G. Lu, K.H. Chen, Z. Bo and J. Chen, *J. Phys. Chem. Lett.*, **2**, 537 (2011); https://doi.org/10.1021/jz200087w
3. S. Lee, K. Lee, C.H. Liu and Z. Zhong, *Nanoscale*, **4**, 639 (2012); https://doi.org/10.1039/C1NR11574J
4. X. Li, X. Wang, L. Zhang, S. Lee and H. Dai, *Science*, **319**, 1229 (2008); https://doi.org/10.1126/science.1150878
5. A.K. Geim and K.S. Novoselov, *Nat. Mater.*, **6**, 183 (2007); https://doi.org/10.1038/nmat1849
6. H. He, J. Klinowski, M. Forster and A. Lerf, *Chem. Phys. Lett.*, **287**, 53 (1998); https://doi.org/10.1016/S0009-2614(98)00144-4
7. H. He, T. Riedl, A. Lerf and J. Klinowski, *J. Phys. Chem.*, **100**, 19954 (1996); https://doi.org/10.1021/jp961563t
8. S. Stankovich, R.D. Piner, X. Chen, N. Wu, S.T. Nguyen and R.S. Ruoff, *J. Mater. Chem.*, **16**, 155 (2006); https://doi.org/10.1039/B512799H
9. S. Niyogi, E. Bekyarova, M.E. Itkis, J.L. McWilliams, M.A. Hamon and R.C. Haddon, *J. Am. Chem. Soc.*, **128**, 7720 (2006); https://doi.org/10.1021/ja060680r
10. J. Nanda, A. Biswas, B. Adhikari and A. Banerjee, *Angew. Chem. Int. Ed.*, **52**, 5041 (2013); https://doi.org/10.1002/anie.201301128
11. A. Biswas and A. Banerjee, *Soft Matter*, **11**, 4226 (2015); https://doi.org/10.1039/C5SM00359H
12. S. Roy, A. Baral and A. Banerjee, *Chem. Eur. J.*, **19**, 14950 (2013); https://doi.org/10.1002/chem.201301655
13. Z. Sui, X. Zhang, Y. Lei and Y. Luo, *Carbon*, **49**, 4314 (2011); https://doi.org/10.1016/j.carbon.2011.06.006
14. Z. Sui, Q. Meng, X. Zhang, R. Ma and B. Cao, *J. Mater. Chem.*, **22**, 8767 (2012); https://doi.org/10.1039/c2jm00055e
15. X. Huang, X. Qi, F. Boey and H. Zhang, *Chem. Soc. Rev.*, **41**, 666 (2012); https://doi.org/10.1039/C1CS15078B
16. C. Huang, H. Bai, C. Li and G. Shi, *Chem. Commun.*, **47**, 4962 (2011); https://doi.org/10.1039/c1cc10412h
17. A. Biswas and A. Banerjee, *Chem. Asian J.*, **9**, 3451 (2014); https://doi.org/10.1002/asia.201402695
18. B. Adhikari, A. Biswas and A. Banerjee, *ACS Appl. Mater. Interfaces*, **4**, 5472 (2012); https://doi.org/10.1021/am301373n
19. L. Huang, C. Li, W. Yuan and G. Shi, *Nanoscale*, **5**, 3780 (2013); https://doi.org/10.1039/c3nr00196b
20. Y. Xu, K. Sheng, C. Li and G. Shi, *ACS Nano*, **4**, 4324 (2010); https://doi.org/10.1021/nn101187z
21. K.Y. Shin, J.Y. Hong and J. Jang, *Chem. Commun.*, **47**, 8527 (2011); https://doi.org/10.1039/c1cc12913a
22. D.W. Wang, F. Li, J. Zhao, W. Ren, Z.-G. Chen, J. Tan, Z.-S. Wu, I. Gentle, G.Q. Lu and H.-M. Cheng, *ACS Nano*, **3**, 1745 (2009); https://doi.org/10.1021/nn900297m
23. N.D. Luong, N. Pahimanolis, U. Hippi, J.T. Korhonen, J. Ruokolainen, L.S. Johansson, J.D. Nam and J. Seppälä, *J. Mater. Chem.*, **21**, 13991 (2011); https://doi.org/10.1039/c1jm12134k
24. X. Xia, J. Tu, Y. Mai, R. Chen, X. Wang, C. Gu and X. Zhao, *Chemistry*, **17**, 10898 (2011); https://doi.org/10.1002/chem.201100727
25. H. Chen, M.B. Müller, K.J. Gilmore, G.G. Wallace and D. Li, *Adv. Mater.*, **20**, 3557 (2008); https://doi.org/10.1002/adma.200800757
26. S. Park, N. Mohanty, J.W. Suk, A. Nagaraja, J. An, R.D. Piner, W. Cai, D.R. Dreyer, V. Berry and R.S. Ruoff, *Adv. Mater.*, **22**, 1736 (2010); https://doi.org/10.1002/adma.200903611
27. F. Liu, S. Song, D. Xue and H. Zhang, *Adv. Mater.*, **24**, 1089 (2012); https://doi.org/10.1002/adma.201104691
28. Y.L. Huang, H.W. Tien, C.C.M. Ma, S.Y. Yang, S.Y. Wu, H.Y. Liu and Y.W. Mai, *J. Mater. Chem.*, **21**, 18236 (2011); https://doi.org/10.1039/c1jm13790e
29. C. Zhu, S. Guo, Y. Fang and S. Dong, *ACS Nano*, **4**, 2429 (2010); https://doi.org/10.1021/nn1002387
30. W. Hummers Jr. and R.E. Offeman, *J. Am. Chem. Soc.*, **80**, 1339 (1958); https://doi.org/10.1021/ja01539a017
31. K. Rosenlehner, B. Schade, C. Böttcher, C.M. Jäger, T. Clark, F.W. Heinemann and A. Hirsch, *Chemistry*, **16**, 9544 (2010); https://doi.org/10.1002/chem.201001150
32. J. Zhang, H. Yang, G. Shen, P. Cheng, J. Zhang and S. Guo, *Chem. Commun.*, **46**, 1112 (2010); https://doi.org/10.1039/B917705A
33. X. Jiao, Y. Qiu, L. Zhang and X. Zhang, *RSC Adv.*, **7**, 52337 (2017); https://doi.org/10.1039/C7RA10809E
34. T.R.B. Ramakrishna, D.P. Killeen, T.D. Nalder, S.N. Marshall, W. Yang and C.J. Barrow, *Appl. Spectrosc.*, **72**, 1764 (2018); https://doi.org/10.1177/0003702818798405